

Hydrogen isotope ratios of leaf wax *n*-alkanes in loess and floodplain deposits in northern China since the Last Glacial Maximum and their paleoclimatic significance

Yangyang Li ^{a,b,*}, Shiling Yang ^{a,b}, Jule Xiao ^{a,b}, Wenyi Jiang ^a, Xiaoxiao Yang ^{a,b}

^a Key Laboratory of Cenozoic Geology and Environment, Institute of Geology and Geophysics, Chinese Academy of Sciences, Beijing 100029, China

^b University of Chinese Academy of Sciences, Beijing 100049, China



ARTICLE INFO

Article history:

Received 15 November 2016

Received in revised form 24 March 2017

Accepted 2 August 2017

Available online 3 August 2017

Keywords:

n-Alkanes

Compound-specific hydrogen isotope composition

East Asian Summer Monsoon

Holocene

Last Glacial Maximum

ABSTRACT

The hydrogen isotopic composition of leaf-wax *n*-alkanes ($\delta D_{n\text{-alkane}}$) is increasingly used as a proxy for estimating δD of past precipitation (δD_p). However, aridity can also affect sedimentary $\delta D_{n\text{-alkane}}$, complicating the interpretation of paleo- $\delta D_{n\text{-alkane}}$ records. In order to evaluate the effects of the complex interactions and balance between precipitation hydrogen isotope composition and aridity on sedimentary $\delta D_{n\text{-alkane}}$ records, we present two $\delta D_{n\text{-alkane}}$ records from the North China Plain and the western Chinese Loess Plateau across a steep east-west climatic gradient in the East Asian Summer Monsoon area since the Last Glacial Maximum. The estimated δD_p changes, based on a present-day relationship between δD_p and rainfall amounts, can explain much of the $\delta D_{n\text{-alkane}}$ variations in the North China Plain, but do not explain the large variations of $\delta D_{n\text{-alkane}}$ in the western Chinese Loess Plateau. Comparison of $\delta D_{n\text{-alkane}}$ records with observed $\delta D_{n\text{-alkane}}$ values in modern plants and published pollen data indicates that changes in vegetation play a minor role in the variations of $\delta D_{n\text{-alkane}}$. Instead, $\delta D_{n\text{-alkane}}$ values are coincident with aridity both temporally and spatially, i.e. the higher $\delta D_{n\text{-alkane}}$ values the drier climate and vice versa. Aridity effects are more evident in the western Chinese Loess Plateau than in the North China Plain. Therefore, on glacial-interglacial scale, sedimentary $\delta D_{n\text{-alkane}}$ records from the North China Plain mostly reflect changes in δD_p values, whereas those from the western Chinese Loess Plateau largely reflect the effects of aridity, mainly due to a greater evapotranspirational deuterium-enrichment caused by a drier climate in the western Chinese Loess Plateau than in the North China Plain. Further calibrations from modern sediments are required to better define the quantitative relationship between the $\delta D_{n\text{-alkane}}$ and climate in northern China.

© 2017 Elsevier B.V. All rights reserved.

1. Introduction

The stable hydrogen isotopic composition (δD) of precipitation is an effective indicator of hydrology and climate dynamics. Hydrogen isotope ratios of plant lipids derive ultimately from precipitation and thus have a great potential to reflect the precipitation δD values (δD_p) (Sternberg, 1988). Among these lipids, leaf wax *n*-alkanes have attracted particular interest as they are abundant in various geological materials and can persist in the environment over hundred millions of years (Dawson et al., 2004). What makes them unique is that their hydrogen atoms are covalently bonded to carbon atoms and have very slow exchange rates in thermally immature sediments (Schimmelman et al., 1999; Sessions et al., 2004; Pedentchouk et al., 2006). Therefore, δD ratios of sedimentary leaf-wax *n*-alkanes ($\delta D_{n\text{-alkane}}$) have been regarded as promising tool for estimating δD values of past precipitation

(Sachse et al., 2004, 2006; Garcin et al., 2012; Feakins et al., 2016; Zech et al., 2011). However, some observations have shown that aridity can also affect sedimentary $\delta D_{n\text{-alkane}}$ (Douglas et al., 2012; Zech et al., 2015), making the interpretation of paleo- $\delta D_{n\text{-alkane}}$ records rather complex. Therefore, it is necessary to evaluate the effects of the complex interactions and balance between precipitation hydrogen isotope composition and aridity on sedimentary $\delta D_{n\text{-alkane}}$ records.

In the East Asian Summer Monsoon area, a pronounced spatial gradient in temperature and precipitation, similar to the present pattern, existed in both glacials and interglacials (Yang and Ding, 2003, 2008, 2014; Yang et al., 2012; Jiang et al., 2013, 2014). This provides a valuable opportunity to clarify the extent to which precipitation hydrogen isotope composition and aridity affect sedimentary $\delta D_{n\text{-alkane}}$ through temporal and spatial comparisons. Here we present two $\delta D_{n\text{-alkane}}$ records from the western Chinese Loess Plateau (CLP) and the North China Plain (NCP) across a steep east-west climatic gradient since the Last Glacial Maximum (LGM). Our aim is to explore the relative importance of precipitation hydrogen isotope composition and aridity in accounting for the spatiotemporal change of $\delta D_{n\text{-alkane}}$ in the East Asian Monsoon region.

* Corresponding author at: 19 BeiTuChengXi Road, Chao Yang District, Beijing 100029, China.

E-mail address: ly-211@mail.igcas.ac.cn (Y. Li).

2. Setting and stratigraphy

Baiyangdian Lake is the largest freshwater lake in the NCP, located in the Hebei province. It consists of more than 100 small and shallow lakes, covering a total area of 366 km². The regional climate is continental semi-arid with warm and wet summers, cold and dry winters. At present, the mean annual temperature and precipitation are 13 °C and 540 mm, respectively. Modern vegetation surrounding the lake is dominated by *Artemisia*, Poaceae and *Aster*. The permanent and seasonal wetlands are predominantly of emergent macrophytes, mainly *Phragmites australis* and *Acorus calamus*.

The study section (38.87°N, 115.90°E) lies ~5 km southwest of Lake Baiyangdian, which has a thickness of 8.4 m (Fig. 1). In general, the lithology of the section can be divided into three units: the lower part consists of yellowish floodplain silt (8.4–3.4 m), the middle part consists of alternatively deposited silt and dark lacustrine clay (3.4–0.4 m), and the upper part is dominated by floodplain soil (0–0.4 m) which has been disturbed by agricultural activities. Two sharp contacts can be observed at the depth of 2.8 m and 1.3 m.

The Jingtai loess section (37.70°N, 104.47°E) is located in the westernmost part of the CLP (Fig. 1). It is characterized by arid climate, with precipitation mainly concentrated in summer. At present, the mean annual temperature is 9.7 °C and the annual precipitation is 102 mm. Vegetation there is dominated by temperate dry steppe.

The Jingtai section consists of the Holocene soil S0 and the upper part of loess unit L1. The Holocene soil, S0, is dark in color because of its relatively high organic matter content. The Loess unit L1, yellowish in color and massive in structure, was deposited during the last glacial period. The L1 loess unit can be generally subdivided into five sub-units, termed L1-1, L1-2, L1-3, L1-4, and L1-5. L1-2 and L1-4 are weakly developed soils, and the others are typical loess horizons. Previous studies have shown that L1-2 was deposited in the late marine isotope stage (MIS) 3, and the L1-1 was deposited in the (MIS) 2 which includes the LGM (Kukla, 1987; Ding et al., 2002; Lu et al., 2007; Yang and Ding, 2014). To ensure that we used a complete cold-warm cycle for *n*-alkane studies, the section was sampled down to loess unit L1-2.

3. Sampling and analytical methods

3.1. Sampling methods

At each site, a ~1–2 m wide vertical trench was excavated along the gully wall, fresh samples were then taken at 5–10 cm intervals. In addition, 9 leaf samples from the dominant species around the Lake Baiyangdian and 1 lake surface sediment sample were also collected in order to constrain the *n*-alkane sources in floodplain deposits. The leaf samples include five terrestrial plants (*Salix* L., *Artemisia capillaris*, *Aster tataricus*, *Imperata cylindrica*, *Setaria viridis*), two submerged species (*Najas* Linn. and *Ceratophyllum demersum*), and two emergent plants (*Phragmites australis* and *Acorus calamus*).

3.2. Grain size measurement

For stratigraphic correlation and time-scale modulation, grain size was measured for all samples using a SALD-3001 laser diffraction particle analyzer. Ultrasonic pretreatment with addition of a 20% solution of (NaPO₃)₆ was used to disperse the samples prior to particle size determination (for details see Ding et al., 1999).

3.3. Chronology

The chronology of the Baiyangdian section was established by 16 radiocarbon ages derived from accelerator mass spectrometry (AMS) dating on bulk organic matter at Paleo Labo Co., Ltd., Japan (Table 1). Three of the dates (PLD-24432, PLD-24439 and PLD-24440) were excluded because they caused an age reversal and decreased the quality of the model. After the removal of outliers, calibration was done in Intcal 7.0.4 program using the INTCAL13 curve (Reimer et al., 2013). The age-depth model was based on linear interpolation between the calibrated radiocarbon dates. Sediment ages above 1.3 m and below 7.95 m were estimated by linear extrapolation of sedimentation rates (Fig. 2). The profile covers the last 35.7 ka B.P. (Fig. 2).

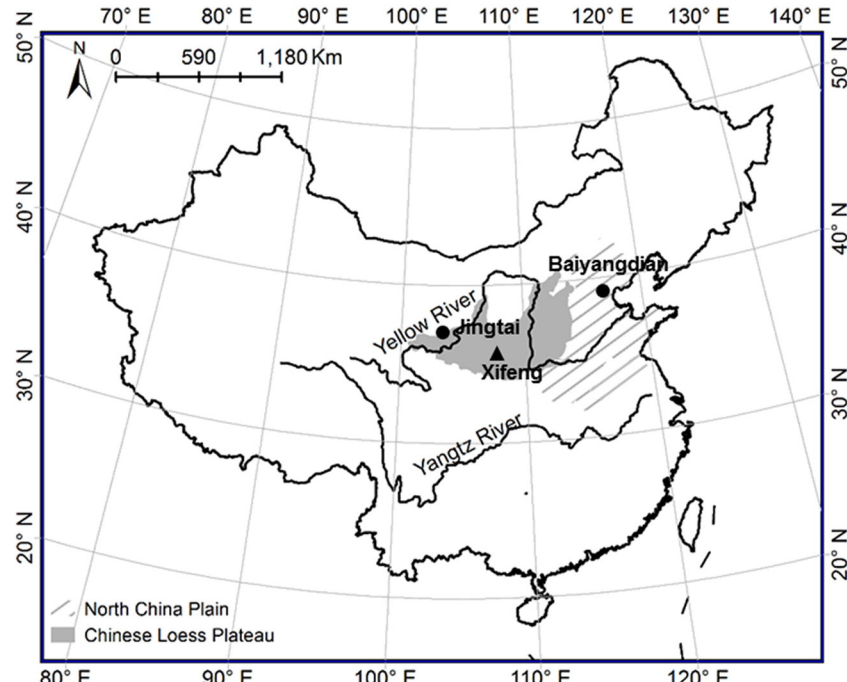


Fig. 1. Map showing study sites in the Chinese Loess Plateau and North China Plain. Solid circles show sites investigated in this study, and the solid triangle denotes the Xifeng section previously studied by Liu and Huang (2005). The arrow indicates the direction of the summer monsoonal winds.

Table 1

Radiocarbon ages of bulk organic matter from the Baiyangdian section.

| Laboratory number | Depth, m | Dating material | ^{14}C age, years B.P. | 2σ cal age, years B.P. | Median cal, years B.P. |
|-------------------|----------|-----------------|---------------------------------|-------------------------------|------------------------|
| PLD-24427 | 1.35 | Bulk sediment | 3380 ± 20 | 3645–3575 | 3620 |
| PLD-24428 | 1.5 | Bulk sediment | 3690 ± 25 | 4090–3965 | 4035 |
| PLD-24429 | 1.7 | Bulk sediment | 4780 ± 25 | 5555–5470 | 5520 |
| PLD-24430 | 1.9 | Bulk sediment | 5320 ± 25 | 6185–6000 | 6090 |
| PLD-24431 | 2 | Bulk sediment | 6000 ± 25 | 6910–6775 | 6840 |
| PLD-24432 | 2.55 | Bulk sediment | 8605 ± 35 | 9635–9525 | 9555 |
| PLD-24433 | 2.95 | Bulk sediment | 8195 ± 30 | 9260–9030 | 9145 |
| PLD-24434 | 3.15 | Bulk sediment | 8840 ± 30 | 9960–9745 | 9925 |
| PLD-24435 | 3.85 | Bulk sediment | $11,340 \pm 35$ | 13,275–13,095 | 13,185 |
| PLD-24436 | 4.45 | Bulk sediment | $13,715 \pm 40$ | 16,795–16,335 | 16,555 |
| PLD-24437 | 5 | Bulk sediment | $17,560 \pm 60$ | 21,465–20,970 | 21,220 |
| PLD-24438 | 5.6 | Bulk sediment | $19,620 \pm 60$ | 23,885–23,400 | 23,640 |
| PLD-24439 | 6.2 | Bulk sediment | $23,890 \pm 80$ | 28,145–27,715 | 27,915 |
| PLD-24440 | 6.8 | Bulk sediment | $21,320 \pm 70$ | 25,850–25,480 | 23,670 |
| PLD-24441 | 7.35 | Bulk sediment | $24,690 \pm 90$ | 28,950–28,475 | 28,720 |
| PLD-24442 | 7.95 | Bulk sediment | $26,540 \pm 110$ | 31,025–30,595 | 30,815 |

The sequence of alternating loess (L1-1) and paleosol (S0) at Jingtai suggests that it covers the Holocene and the LGM period, which is supported by the radiocarbon dating results (S. Yang et al., 2015a; X. Yang et al., 2015b). The age scale was established by correlating our grain-size data with Chinese Loess Millennial-scale Oscillation Stack (CHILOMOS) (Yang and Ding, 2014). A total of 4 age control points were used, namely the boundaries of L1-2/L1-1 (27 ka) and L1-1/S0 (11 ka), the coarsest part of L1-1 (18 ka), and the finest part of S0 (6 ka). Ages for other samples were based on linear interpolation by assuming a uniform depositional rate between these time controls. This sequence covers a period of 34.9 ka (Fig. 3).

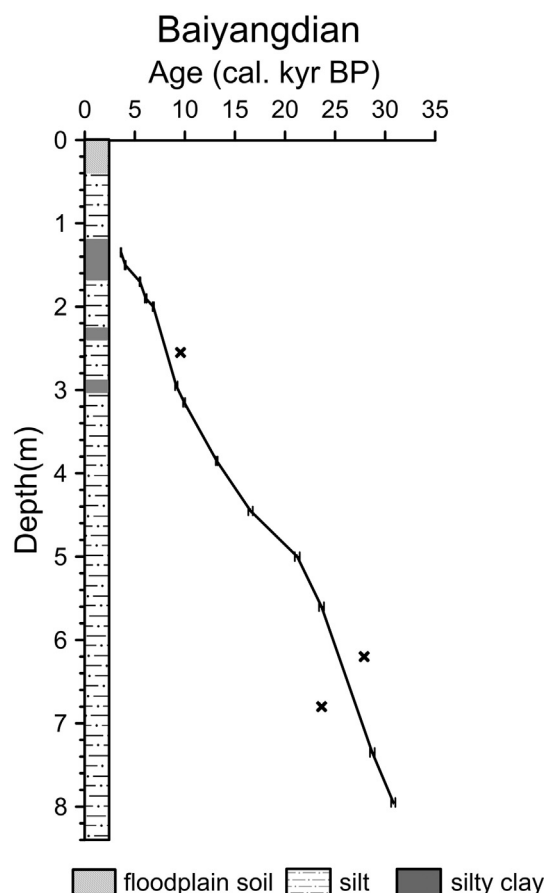


Fig. 2. Age model for the Baiyangdian section. The error bars represent the range of calibrated ages, and the crosses indicate the outliers.

3.4. n-Alkane extraction, purification and quantitation

Approximately 20–60 g of freeze-dried, finely ground sediment was extracted using an Accelerated Solvent Extractor (ASE350, Dionex) with dichloromethane:methanol (9:1 v/v) at 100 °C and 1500 psi. Leaf samples (0.5–1 g) were freeze-dried, cut into pieces with solvent cleaned scissors and ultrasonically extracted with dichloromethane. Lipid extracts were dried under a stream of N₂. Hydrocarbon fractions were obtained using silica column chromatography by elution with hexane. n-Alkanes were further purified from cyclic and branched alkanes using urea adduction.

n-Alkanes were identified and quantified using an Agilent 6890 gas chromatograph (GC) equipped with a flame ionization detector (FID). An HP-1MS capillary column (60 m × 0.32 mm × 0.25 μm) was used with Helium as the carrier gas at a flow of 1.0 ml/min. The GC oven temperature was programmed from 40 °C to 150 °C at 10 °C/min and then 150 °C to 310 °C (held 20 min) at 6 °C/min. n-Alkanes were identified through comparison of elution times with known n-alkane standards.

3.5. n-Alkane hydrogen isotope analysis

Hydrogen isotope analyses were performed using a Thermo Scientific Trace GC Ultra coupled to a Thermo Scientific Delta V Advantage isotope ratio mass spectrometer with a high-temperature conversion system operating at 1430 °C. GC column, carrier flow, and ramp conditions for 8D analyses were identical to the above. The H₃⁺ factor was determined daily and was 1.83 ± 0.01 (1σ , $n = 15$) during sample analysis, ensuring stable ion source conditions. Reproducibility and accuracy were evaluated using standards containing six n-alkanes ($n\text{-C}_{21}$, $n\text{-C}_{23}$, $n\text{-C}_{25}$, $n\text{-C}_{27}$, $n\text{-C}_{29}$, $n\text{-C}_{31}$) after every six sample analyses. The precision (1σ) for the six laboratory standards was $\pm 3\%$ throughout the entire process. Values are reported using standard delta notation (δD) as per mil (‰) deviations from Vienna standard mean ocean water (VSMOW).

4. Results

4.1. Grain size

Grain size records exhibit distinct variations at glacial–interglacial scales (Fig. 3). Overall, loess unit L1-1 at Jingtai and glacial silt unit at Baiyangdian show coarse grain size, while paleosol S0 at Jingtai and the Holocene unit of silt interbedded with clay at Baiyangdian are characterized by fine particle sizes. In the Baiyangdian section, the median

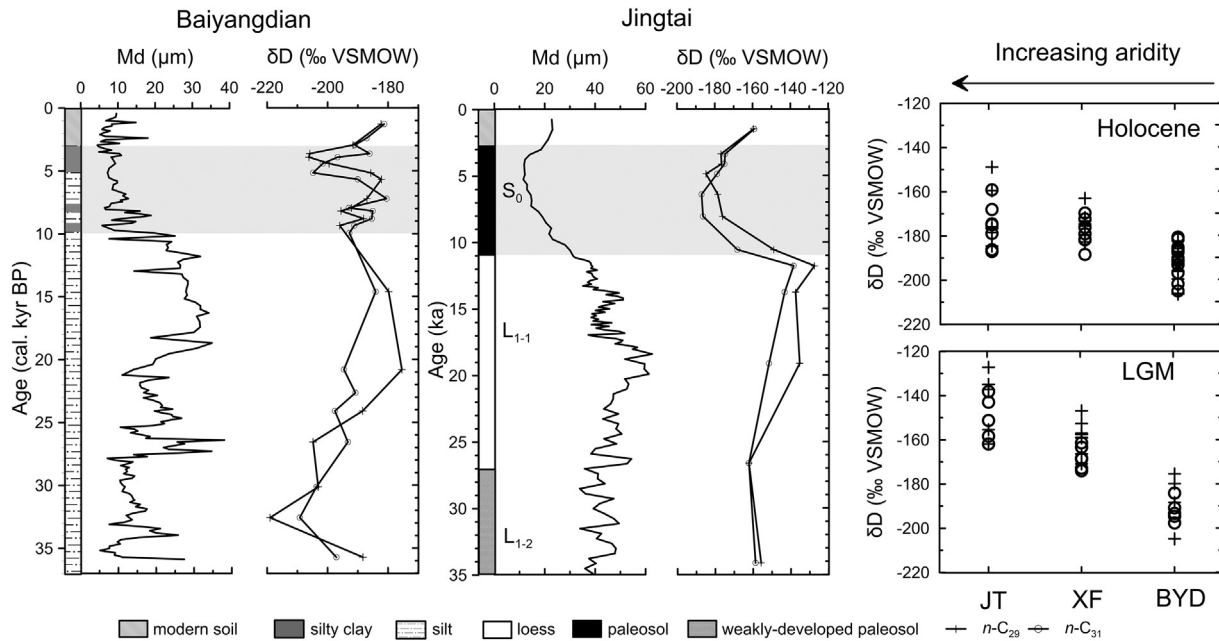


Fig. 3. Temporal and spatial changes of δD values at Baiyangdian and Jingtai. The shaded zones indicate the Holocene Optimum, and data for Xifeng (XF) comes from Liu and Huang (2005).

grain size values are 5–39 μm for glacial sediments, and 7–24 μm for the Holocene deposits. The Holocene deposits exhibit smaller amplitude fluctuations than glacial deposits, implying more stable hydrodynamic conditions in the Holocene. In the Jingtai section, the median grain size falls in the range 35–60 μm for loess units L1-1, and 10–20 μm for the Holocene soil S0.

4.2. *n*-Alkane distributions

In order to better constrain the source of leaf wax *n*-alkanes in floodplain deposits, we compared the *n*-alkane distributions of modern plants with those of sediments (Fig. 4). The *n*-alkanes exhibited significant differences in distribution between terrestrial and aquatic species.

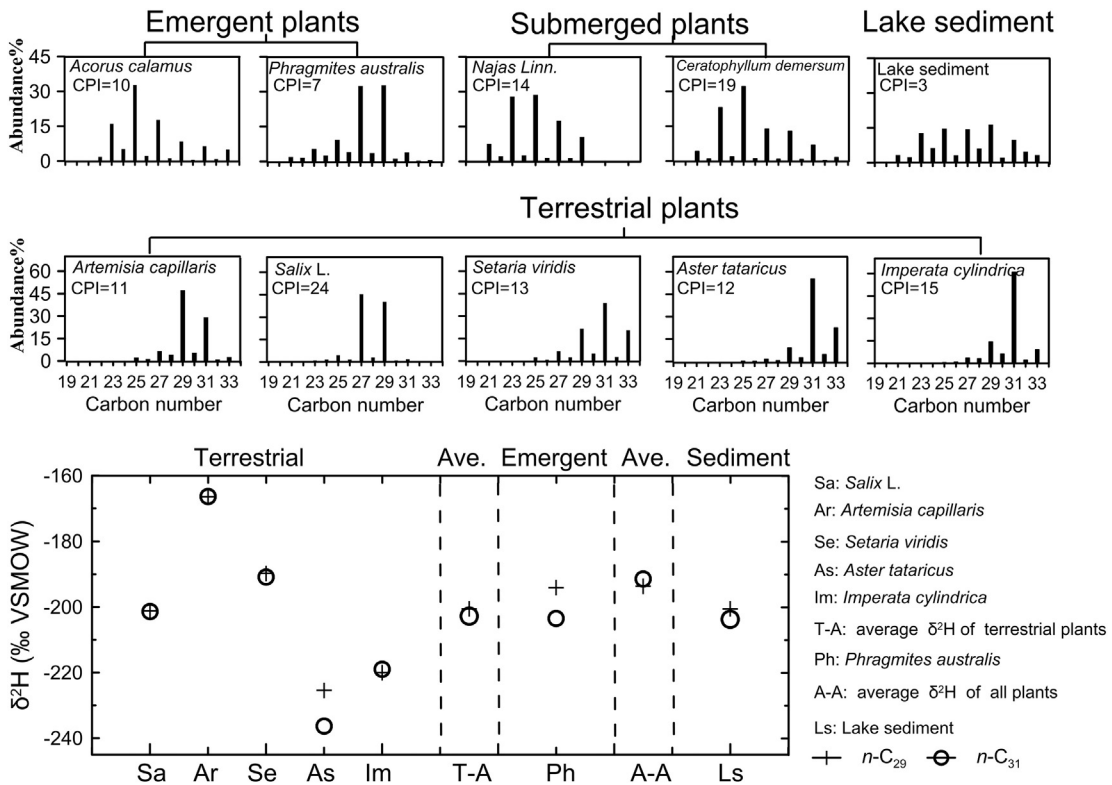


Fig. 4. *n*-Alkane distributions and hydrogen isotope ratios of leaf waxes collected around Lake Baiyangdian. The associated Carbon Preference Index (CPI) was calculated using the following formula (Bray and Evans, 1961): CPI = $\frac{1}{2} \frac{(C_{25} + C_{27} + C_{29} + C_{31} + C_{33}) + (C_{26} + C_{28} + C_{30} + C_{32})}{(C_{24} + C_{26} + C_{28} + C_{30} + C_{32} + C_{34})}$, (1), where C_x is the concentration of the *n*-alkane (C) with x carbons.

Terrestrial plants were found to mainly produce $n\text{-C}_{27}\text{--}n\text{-C}_{33}$ with $n\text{-C}_{29}$ or $n\text{-C}_{31}$ as the most abundant n -alkanes, while aquatic species produced $n\text{-C}_{19}\text{--}n\text{-C}_{25}$ with $n\text{-C}_{23}$ or $n\text{-C}_{25}$ as the most abundant n -alkanes, except *Phragmites australis*, which contained abundant $n\text{-C}_{27}$ and $n\text{-C}_{29}$. Modern surface sediment produced n -alkanes with 19–35 carbon atoms and contained $n\text{-C}_{29}$ as the predominant n -alkane. There is a strong odd-over-even predominance in all samples, and the CPI (Carbon Preference Index) values range from 3 to 24.

n -Alkanes at Baiyangdian are dominated by $n\text{-C}_{21}\text{--}n\text{-C}_{33}$ with $n\text{-C}_{29}$ or $n\text{-C}_{31}$ as the most abundant compounds, showing a pattern similar to that of the modern surface sediment, and their CPI values vary between 2 and 8. In the Jingtai section, all samples show n -alkane distributions dominated by $n\text{-C}_{25}\text{--}n\text{-C}_{33}$ with the most abundant being $n\text{-C}_{27}$ or $n\text{-C}_{29}$ or $n\text{-C}_{31}$, and CPI values range from 3 to 10.

4.3. n -Alkane hydrogen isotope ratios

In this study, we focus on the δD of the $n\text{-C}_{29}$ and $n\text{-C}_{31}$ n -alkane as they are usually abundant in terrestrial plant-waxes and have the highest concentration in most of our samples. Interestingly, we find that *Phragmites australis* also has abundant $n\text{-C}_{29}$, similar to terrestrial plants. To evaluate the potential effects of *Phragmites australis* on the δD values of floodplain deposits, a comparison of δD values was made among *Phragmites australis*, terrestrial species and surface sediment (Fig. 4). δD_{C29} and δD_{C31} values of terrestrial species range from $-225.4\text{\textperthousand}$ to $-166.5\text{\textperthousand}$, and $-236.3\text{\textperthousand}$ to $-166.4\text{\textperthousand}$, respectively. Specifically, *Artemisa* yields the highest δD_{C29} and δD_{C31} values, whereas *Aster* has the lowest δD_{C29} and δD_{C31} values. Intermediate values are found in *Salix L.*, *Setaria viridis* and *Imperata cylindrical*. *Phragmites australis* has δD_{C29} and δD_{C31} values ($-194.1\text{\textperthousand}$ and $-203.5\text{\textperthousand}$) similar to the terrestrial average (δD_{C29} of $-200.6\text{\textperthousand}$ and δD_{C31} of $-202.8\text{\textperthousand}$). For lake surface sediment, δD_{C29} and δD_{C31} values are similar to the average of all studied species.

Fig. 3 illustrates the temporal and spatial changes of $\delta D_{n\text{-alkane}}$ values at Baiyangdian and Jingtai. The $\delta D_{n\text{-alkane}}$ records from both Baiyangdian and Jingtai show an overall decreasing trend from the LGM to the Holocene, consistent with previous results from Xifeng (Liu and Huang, 2005). In the Baiyangdian section, δD_{C29} and δD_{C31} values varied between $-219.0\text{\textperthousand}$ and $-175.4\text{\textperthousand}$, and $-209.2\text{\textperthousand}$ and $-184.1\text{\textperthousand}$, respectively. Values remained low between 36 and 30 ka B.P., and then gradually increased and reached their peaks around $\sim 20\text{--}15$ ka B.P., followed by a gradual decline. In the Jingtai section, δD_{C29} and δD_{C31} values range from -184.6 to -127.2 , and -187.0 to -138.2 , respectively. δD values were much higher during the LGM than the Holocene and the late MIS 3. There is a greater glacial deuterium-enrichment (D -enrichment) relative to the Holocene in Jingtai than in Baiyangdian.

In order to identify the spatial pattern, a transect from east to west was established (Baiyangdian-Xifeng-Jingtai) by combining our results with published data from the Xifeng section (Liu and Huang, 2005). From east to west along the transect, δD_{C29} and δD_{C31} generally showed a gradual increase for both the LGM and Holocene deposits (Fig. 3).

5. Discussion

5.1. Sources of n -alkanes

Previous studies have suggested that n -alkanes ranging from $n\text{-C}_1$ to $n\text{-C}_{31}$ with $n\text{-C}_{21}$, $n\text{-C}_{23}$ or $n\text{-C}_{25}$ being the most abundant compounds are derived from submerged and floating plants (Ficken et al., 2000). Our results from submerged plants are consistent with this finding. Therefore medium chain n -alkanes ($n\text{-C}_{21}\text{--}n\text{-C}_{25}$) in the Baiyangdian section are mainly derived from submerged and/or floating plants. Terrestrial species around Lake Baiyangdian are characterized by a predominance of long chain n -alkanes ($n\text{-C}_{27}\text{--}n\text{-C}_{33}$) with a strong odd-over-even carbon chain preference, in a good agreement with previous studies (Eglinton and Hamilton, 1967). Interestingly, *Phragmites*

australis has a distribution similar to terrestrial plants. As such, the long-chain n -alkanes ($n\text{-C}_{25}\text{--}n\text{-C}_{33}$) in the Baiyangdian section are likely derived from terrestrial plants and *Phragmites australis*. In the Jingtai section, n -alkanes in all samples are dominated by long chain n -alkanes ($n\text{-C}_{25}\text{--}n\text{-C}_{33}$). Given *Phragmites australis* rarely exists on the arid Loess Plateau, long chain n -alkanes in loess deposits are mainly derived from terrestrial plants.

5.2. Environmental controls on $\delta D_{n\text{-alkane}}$

The three main factors controlling the $\delta D_{n\text{-alkane}}$ values, namely the precipitation δD values, vegetation type and evaporative D -enrichment of leaf and soil water induced by aridity, are discussed in detail as below.

5.2.1. Moisture source

Precipitation in northern China is mainly controlled by the East Asian Summer Monsoon, which transports heat and moisture from the equatorial Pacific Ocean to the Asian continental interior. Since most precipitation concentrates in summer, the stable isotopic composition of precipitation thus shows a strong seasonal variation in response to the seasonal temperature and rainfall amounts change (Yang et al., 2012). In the summer monsoon domain, low $\delta^{18}\text{O}$ values of precipitation occur in summer due to amount effect, while in arid region high $\delta^{18}\text{O}$ values of precipitation occur in summer due to temperature effect (Araguás-Araguás et al., 1998; Johnson and Ingram, 2004; Vuille et al., 2005; Yang et al., 2012). For the study area located in the marginal zones of the summer monsoon, precipitation isotope values exhibit dependence on both temperature and amount of precipitation (Araguás-Araguás et al., 1998; Johnson and Ingram, 2004). As shown in Fig. 5, high δD_p values occur in summer but with a distinct dip during July to September in the monsoon-influenced eastern sites (IAEA/WMO, 2016).

On glacial-interglacial timescales, in addition to temperature and rainfall amount effects, moisture source could also affect the isotopic composition of precipitation. During the LGM, the increased ice volume would have made global seawater isotopically heavier as the lighter isotope is preferentially incorporated into the ice sheet. $\delta^{18}\text{O}$ in the South China sea (moisture source for EASM) at the LGM would be $\sim 1.5\text{\textperthousand}$ more enriched than present as indicated by benthic foraminifer record (Tian et al., 2002). Using the global meteoric water line and assuming the deuterium excess remained constant between the LGM and the Holocene, this is equivalent to a δD enrichment of $\sim 12\text{\textperthousand}$ (Craig, 1961; Dansgaard, 1964; Rozanski et al., 1992). Changes in the amount effect could have potentially led to an increase of $\sim 1\text{\textperthousand}$ in $\delta^{18}\text{O}$ values at the LGM. This is based on a modern δD -rainfall amount relationship: $\beta_{\log P} = d\delta^{18}\text{O} / d\log P$, with a maximum $\beta_{\log P}$ for the summer monsoon marginal zone of ~ 4 (Johnson and Ingram, 2004) and a reduction in precipitation of $\sim 40\%$ (Jiang et al., 2011). The equivalent increase in δD value was about 8\textperthousand . Taken together, the δD_p during the LGM would have been $20\text{\textperthousand}$ more enriched than the Holocene as a result of the amount effect and ice volume changes. This explains much of the variability in $\delta D_{n\text{-alkane}}$ of Baiyangdian ($\sim 21\text{\textperthousand}$) but does not explain the observed $\sim 49\text{--}57\text{\textperthousand}$ $\delta D_{n\text{-alkane}}$ fluctuations at Jingtai. In addition, given the temperature effect would have led to more depleted δD_p values during the LGM, which would counteract some of the enriched δD_p values caused by ice volume and rainfall amount effects, the actual LGM-Holocene δD_p shift is likely to be much smaller. It is thus indicated that the precipitation δD_p appears to be the primary control on $\delta D_{n\text{-alkane}}$ at Baiyangdian, but factors other than δD_p may exert important influences on $\delta D_{n\text{-alkane}}$ at Jingtai.

5.2.2. Vegetation type

The sedimentary record integrates inputs from many vegetation sources. There are considerable difference in $\delta D_{n\text{-alkane}}$ values for different plant types grown under similar conditions, due to differences in plant morphology, water use efficiency and biochemistry. For example,

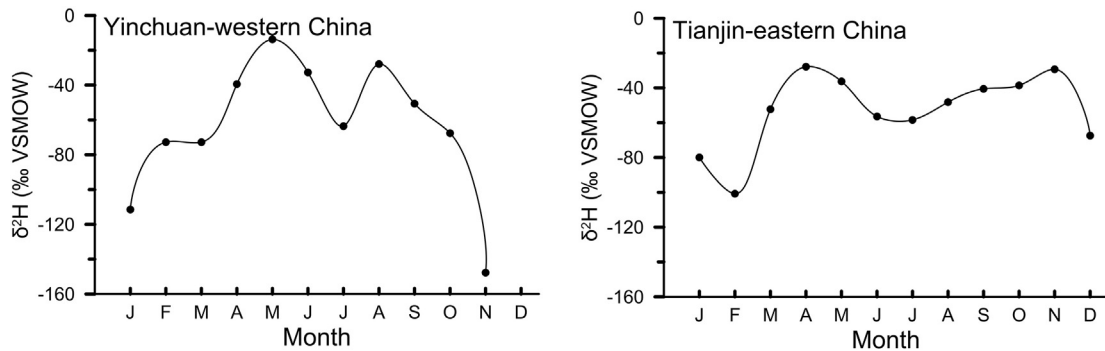


Fig. 5. Seasonal variations of mean weighted δD_p (VSMOW) for Yinchuan (left) and Tianjin (right) in the summer monsoon marginal zone (IAEA/WMO, 2016).

C_4 monocots are ~15% more D-enriched than C_3 monocots, and C_3 monocots are D-depleted by ~36% than C_3 dicots (Chikaraishi and Naraoka, 2003; Chikaraishi et al., 2004; Liu et al., 2006; Smith and Freeman, 2006; McInerney et al., 2011; Sachse et al., 2012). Hence, vegetation effects should be taken into account when interpreting sedimentary $\delta D_{n\text{-alkane}}$ records.

Long-chain n -alkanes at Baiyangdian are mainly derived from terrestrial plants and *Phragmites australis*. Previous studies found that lakes with abundant emergent aquatic plants, which likely rely on groundwater sources, showed more negative δD values than lakes without abundant emergent aquatic plants (Shuman et al., 2006). However, *Phragmites australis* present here has similar $\delta D_{n\text{-alkane}}$ values to the average of the terrestrial species. Therefore, changes in *Phragmites australis* likely exert little influence on the variations of $\delta D_{n\text{-alkane}}$ values. Pollen records have shown that steppe vegetation prevailed in Baiyangdian since the LGM, while broadleaf trees increased during the Holocene (Xu and Wu, 1986). Since trees have been shown to have higher $\delta D_{n\text{-alkane}}$ values than grasses grown on similar conditions (Hou et al., 2007; Liu and Yang, 2008; Sachse et al., 2012), the $\delta D_{n\text{-alkane}}$ values are expected to be higher in the Holocene than in the LGM. On the contrary, higher $\delta D_{n\text{-alkane}}$ values are observed in the LGM (Fig. 4). Thus changes in trees may play a minor role in the variations of $\delta D_{n\text{-alkane}}$ values.

Pollen and stable carbon isotope records from Jingtai have shown that C_3 grass prevailed both in the LGM and the Holocene, and shrubs such as *Echinops*-type and *Chenopodiaceae*, increased in the LGM (S. Yang et al., 2015a; X. Yang et al., 2015b). Shrubs are generally D-enriched by ~50% than C_3 grass grown on similar conditions (Chikaraishi and Naraoka, 2003; Smith and Freeman, 2006; Sachse et al., 2012). If shrub changes were the major control on $\delta D_{n\text{-alkane}}$, then the ~49%–57% variations of $\delta D_{n\text{-alkane}}$ would have resulted from a total replacement of C_3 grasses with shrubs at Jingtai. However, pollen of shrubs increased to no more than ~20% throughout the study interval (X. Yang et al., 2015b). It is thus suggested that the changes in the species of steppe vegetation may play a minor role in the large variations of $\delta D_{n\text{-alkane}}$ values for Chinese loess.

5.2.3. Aridity

Aridity exerts a control on the extent of evapotranspiration of soil-water and leaf-water. In arid environments, soil and leaf water become deuterium-enriched by evapotranspiration, leading to higher $\delta D_{n\text{-alkane}}$ values (Feehins and Sessions, 2010; Smith and Freeman, 2006; McInerney et al., 2011). Modern observations from southeastern Mexico and northern Central America indicated that changes in aridity can cause large variability in leaf wax δD values that is independent of δD_p (Douglas et al., 2012). Aridity is also recognized as an important cause for $\delta D_{n\text{-alkane}}$ variability in loess (Liu and Huang, 2005; Zech et al., 2013). Thus, aridity effects need to be carefully evaluated when interpreting paleo- $\delta D_{n\text{-alkane}}$ records.

Our results showed that 1) $\delta D_{n\text{-alkane}}$ values were higher in the LGM than in the Holocene and the late MIS 3 in both sections, in accordance

with a drier climate in the LGM than in the Holocene and the late MIS 3; and 2) from east to west along the transect, the $\delta D_{n\text{-alkane}}$ values exhibited an overall westward increase in both the LGM and the Holocene deposits, coinciding with the present spatial climatic gradient, namely a westward increase in aridity. This relationship indicates that aridity significantly influences $\delta D_{n\text{-alkane}}$ values. Our study further demonstrated that there is a greater glacial D-enrichment relative to the Holocene in Jingtai than in Baiyangdian, suggesting aridity effects are more evident in Jingtai than in Baiyangdian. Furthermore, the estimated δD_p changes could explain much of $\delta D_{n\text{-alkane}}$ variations at Baiyangdian, but do not explain the large variations of $\delta D_{n\text{-alkane}}$ at Jingtai. It is thus suggested that $\delta D_{n\text{-alkane}}$ at Baiyangdian is mainly controlled by δD_p , which is consistent with the previous findings from the surface soil in Eastern China (Rao et al., 2009), while $\delta D_{n\text{-alkane}}$ at Jingtai is mainly controlled by aridity, with δD_p exerting a secondary influence. This is probably due to the drier climate at Jingtai would lead to more D-enrichment from transpiration and soil evaporation than at Baiyangdian.

Therefore, $\delta D_{n\text{-alkane}}$ values from east region may provide estimates for the isotopic composition of paleoprecipitation, while $\delta D_{n\text{-alkane}}$ records from west region have a great potential to provide a measure of the evaporative enrichment and a paleo-aridity index. Further calibrations from modern sediments are required to better define the quantitative relationship between the $\delta D_{n\text{-alkane}}$ and climate in northern China.

6. Conclusions

Hydrogen isotopic ratios of leaf-wax n -alkanes from loess and floodplain sediments since the Last Glacial Maximum were evaluated across a marked aridity gradient in northern China. The estimated precipitation δD changes can partially explain much of the $\delta D_{n\text{-alkane}}$ variations in the NCP but do not explain the relatively large variations in the western CLP. Changes in vegetation play a minor role on $\delta D_{n\text{-alkane}}$, as indicated by pollen records and modern observations. Instead, aridity shows a good coincidence with $\delta D_{n\text{-alkane}}$ values both temporally and spatially, i.e. the higher $\delta D_{n\text{-alkane}}$ values the drier climate and vice versa. Aridity effects are more evident in the western CLP than in the NCP. It is thus suggested that precipitation δD values and aridity have distinct impacts on sedimentary $\delta D_{n\text{-alkane}}$ records in northern China, whereas their relative impacts are spatially different, with a relatively stronger aridity effects in the western CLP and a more dominate precipitation δD influence in the NCP. This may be caused by more D-enrichment through leaf water transpiration and soil water evaporation in the western CLP under drier conditions. These findings indicate that sedimentary $\delta D_{n\text{-alkane}}$ records from the west region have a great potential to indicate aridity, while $\delta D_{n\text{-alkane}}$ records from the east region largely reflect δD values of precipitation.

Acknowledgements

This study was supported by the National Natural Science Foundation of China (Grant No. 41672175), the National Basic Research

Program of China Grants (2015CB953804), and the “Strategic Priority Research Program” of the Chinese Academy of Sciences (Grant No. XDB03020503). We thank Qinghai Xu, Rulin Wen, Dayou Zhai, and Jiawei Fan for the assistance in the field, and Weiguo Liu, Xu Wang, Yunning Cao, Zhenghao Zhao, and Weijuan Sheng for help in the laboratory and for valuable discussions. We are grateful to two anonymous reviewers for their constructive comments and to Paul Hesse for editorial handling.

References

- Araguás-Araguás, L., Froehlich, K., Rozanski, K., 1998. Stable isotope composition of precipitation over southeast Asia. *J. Geophys. Res. Atmos.* 103, 28721–28742.
- Bray, E.E., Evans, E.D., 1961. Distribution of n-paraffins as a clue to recognition of source beds. *Geochim. Cosmochim. Acta* 22, 1–15.
- Chikaraishi, Y., Naraoka, H., 2003. Compound-specific δD - $\delta^{13}\text{C}$ analyses of n-alkanes extracted from terrestrial and aquatic plants. *Phytochemistry* 63, 361–371.
- Chikaraishi, Y., Naraoka, H., Poulsen, S.R., 2004. Hydrogen and carbon isotopic fractionations of lipid biosynthesis among terrestrial (C_3 , C_4 and CAM) and aquatic plants. *Phytochemistry* 65, 1369–1381.
- Craig, H., 1961. Isotopic variations in meteoric waters. *Science* 133, 1702–1703.
- Dansgaard, W., 1964. Stable isotopes in precipitation. *Tellus* 16, 436–468.
- Dawson, D., Grice, K., Wang, S.X., Alexander, R., Radke, J., 2004. Stable hydrogen isotopic composition of hydrocarbons in torbanites (Late Carboniferous to Late Permian) deposited under various climatic conditions. *Org. Geochem.* 35, 189–197.
- Ding, Z.L., Ren, J.Z., Yang, S.L., Liu, T.S., 1999. Climate instability during the penultimate glaciation: evidence from two high-resolution loess records, China. *J. Geophys. Res. Atmos.* 104, 20123–20132.
- Ding, Z., Derbyshire, E., Yang, S., Yu, Z., Xiong, S., Liu, T., 2002. Stacked 2.6-Ma grain size record from the Chinese loess based on five sections and correlation with the deep-sea $\delta^{18}\text{O}$ record. *Paleoceanography* 17.
- Douglas, P.M., Pagani, M., Brenner, M., Hodell, D.A., Curtis, J.H., 2012. Aridity and vegetation composition are important determinants of leaf-wax δD values in southeastern Mexico and Central America. *Geochim. Cosmochim. Acta* 97, 24–45.
- Eglinton, G., Hamilton, R.J., 1967. Leaf epicuticular waxes. *Science* 156, 1322–1335.
- Feehins, S.J., Sessions, A.L., 2010. Controls on the D/H ratios of plant leaf waxes in an arid ecosystem. *Geochim. Cosmochim. Acta* 74, 2128–2141.
- Feehins, S.J., Bentley, L.P., Salinas, N., Shenkin, A., Blonder, B., Goldsmith, G.R., Ponton, C., Arvin, L.J., Wu, M.S., Peters, T., West, A.J., Martin, R.E., Enquist, B.J., Asner, G.P., Malhi, Y., 2016. Plant leaf wax biomarkers capture gradients in hydrogen isotopes of precipitation from the Andes and Amazon. *Geochim. Cosmochim. Acta* 182, 155–172.
- Ficken, K.J., Li, B., Swain, D., Eglinton, G., 2000. An n-alkane proxy for the sedimentary input of submerged/floating freshwater aquatic macrophytes. *Org. Geochem.* 31, 745–749.
- Garcin, Y., Schwab, V.F., Gleixner, G., Kahmen, A., Todou, G., Séne, O., Onana, J.-M., Achoudong, G., Sachse, D., 2012. Hydrogen isotope ratios of lacustrine sedimentary n-alkanes as proxies of tropical African hydrology: insights from a calibration transect across Cameroon. *Geochim. Cosmochim. Acta* 79, 106–126.
- Hou, J., D'Andrea, W.J., MacDonald, D., Huang, Y., 2007. Hydrogen isotopic variability in leaf waxes among terrestrial and aquatic plants around Blood Pond, Massachusetts (USA). *Org. Geochem.* 38, 977–984.
- IAEA/WMO, 2016. Global network of isotopes in precipitation. The GNIP Database. <http://www.iaea.org/water> (downloaded 25-October-2016).
- Jiang, D., Lang, X., Tian, Z., Guo, D., 2011. Last glacial maximum climate over China from PMIP simulations. *Palaeogeogr. Palaeoclimatol. Palaeoecol.* 309, 347–357.
- Jiang, W., Cheng, Y., Yang, X., Yang, S., 2013. Chinese Loess Plateau vegetation since the Last Glacial Maximum and its implications for vegetation restoration. *J. Appl. Ecol.* 50, 440–448.
- Jiang, W., Yang, X., Cheng, Y., 2014. Spatial patterns of vegetation and climate on the Chinese Loess Plateau since the Last Glacial Maximum. *Quat. Int.* 334, 52–60.
- Johnson, K.R., Ingram, B.L., 2004. Spatial and temporal variability in the stable isotope systematics of modern precipitation in China: implications for paleoclimate reconstructions. *Earth Planet. Sci. Lett.* 220, 365–377.
- Kukla, G., 1987. Loess stratigraphy in central China. *Quat. Sci. Rev.* 6, 191–219.
- Liu, W., Huang, Y., 2005. Compound specific D/H ratios and molecular distributions of higher plant leaf waxes as novel paleoenvironmental indicators in the Chinese Loess Plateau. *Org. Geochem.* 36, 851–860.
- Liu, W., Yang, H., 2008. Multiple controls for the variability of hydrogen isotopic compositions in higher plant n-alkanes from modern ecosystems. *Glob. Chang. Biol.* 14, 2166–2177.
- Liu, W., Yang, H., Li, L., 2006. Hydrogen isotopic compositions of n-alkanes from terrestrial plants correlate with their ecological life forms. *Oecologia* 150, 330–338.
- Lu, Y., Wang, X., Wintle, A.C., 2007. A new OSL chronology for dust accumulation in the last 130,000 yr for the Chinese Loess Plateau. *Quat. Res.* 67, 152–160.
- McInerney, F.A., Helliker, B.R., Freeman, K.H., 2011. Hydrogen isotope ratios of leaf wax n-alkanes in grasses are insensitive to transpiration. *Geochim. Cosmochim. Acta* 75, 541–554.
- Pedentchouk, N., Freeman, K.H., Harris, N.B., 2006. Different response of δD values of n-alkanes, isoprenoids, and kerogen during thermal maturation. *Geochim. Cosmochim. Acta* 70, 2063–2072.
- Rao, Z., Zhu, Z., Jia, G., Henderson, A.C.G., Xue, Q., Wang, S., 2009. Compound specific δD values of long chain n-alkanes derived from terrestrial higher plants are indicative of the δD of meteoric waters: evidence from surface soils in eastern China. *Org. Geochem.* 40, 922–930.
- Reimer, P.J., Bard, E., Bayliss, A., Beck, J.W., Blackwell, P.G., Bronk Ramsey, C., Buck, C.E., Cheng, H., Edwards, R.L., Friedrich, M., 2013. IntCal13 and Marine13 radiocarbon age calibration curves 0–50,000 years cal BP. *Radiocarbon* 55, 1869–1887.
- Rozanski, K., Araguás-Araguás, L., Gonfiantini, R., 1992. Relation between long-term trends of oxygen-18 isotope composition of precipitation and climate. *Science* 258, 981–985.
- Sachse, D., Radke, J., Gleixner, G., 2004. Hydrogen isotope ratios of recent lacustrine sedimentary n-alkanes record modern climate variability. *Geochim. Cosmochim. Acta* 68, 4877–4889.
- Sachse, D., Radke, J., Gleixner, G., 2006. δD values of individual n-alkanes from terrestrial plants along a climatic gradient – implications for the sedimentary biomarker record. *Org. Geochem.* 37, 469–483.
- Sachse, D., Billault, I., Bowen, G.J., Chikaraishi, Y., Dawson, T.E., Feakins, S.J., Freeman, K.H., Magill, C.R., McInerney, F.A., van der Meer, M.T.J., Polissar, P., Robins, R.J., Sachs, J.P., Schmidt, H.-L., Sessions, A.L., White, J.W.C., West, J.B., Kahmen, A., 2012. Molecular paleohydrology: interpreting the hydrogen-isotopic composition of lipid biomarkers from photosynthesizing organisms. *Annu. Rev. Earth Planet. Sci.* 40, 221–249.
- Schimmel, A., Lewan, M.D., Wintsch, R.P., 1999. D/H isotope ratios of kerogen, bitumen, oil, and water in hydrous pyrolysis of source rocks. *Geochim. Cosmochim. Acta* 63, 3751–3766.
- Sessions, A.L., Sylva, S.P., Summons, R.E., Hayes, J.M., 2004. Isotopic exchange of carbon-bound hydrogen over geologic timescales. *Geochim. Cosmochim. Acta* 68, 1545–1559.
- Shuman, B., Huang, Y., Newby, P., Wang, Y., 2006. Compound-specific isotopic analyses track changes in seasonal precipitation regimes in the Northeastern United States at ca 8200 cal yr BP. *Quat. Sci. Rev.* 25, 2992–3002.
- Smith, F.A., Freeman, K.H., 2006. Influence of physiology and climate on δD of leaf wax n-alkanes from C_3 and C_4 grasses. *Geochim. Cosmochim. Acta* 70, 1172–1187.
- Sternberg, Ld.S.L., 1988. D/H ratios of environmental water recorded by D/H ratios of plant lipids. *Nature* 333, 59–61.
- Tian, J., Wang, P., Cheng, X., Li, Q., 2002. Astronomically tuned Plio-Pleistocene benthic $\delta^{18}\text{O}$ record from South China Sea and Atlantic-Pacific comparison. *Earth Planet. Sci. Lett.* 203, 1015–1029.
- Vuille, M., Werner, M., Bradley, R.S., Keimig, F., 2005. Stable isotopes in precipitation in the Asian monsoon region. *J. Geophys. Res.* 110.
- Xu, Q., Wu, C., 1986. A preliminary study of the environment in Lake Baiyangdian during the Holocene. *Geogr. Geol.* 5, 51–56.
- Yang, S., Ding, Z., 2003. Color reflectance of Chinese loess and its implications for climate gradient changes during the last two glacial-interglacial cycles. *Geophys. Res. Lett.* 30.
- Yang, S., Ding, Z., 2008. Advance-retreat history of the East-Asian summer monsoon rainfall belt over northern China during the last two glacial-interglacial cycles. *Earth Planet. Sci. Lett.* 274, 499–510.
- Yang, S., Ding, Z., 2014. A 249 kyr stack of eight loess grain size records from northern China documenting millennial-scale climate variability. *Geochem. Geophys. Geosyst.* 15, 798–814.
- Yang, S., Ding, Z., Wang, X., Tang, Z., Gu, Z., 2012. Negative $\delta^{18}\text{O}$ - $\delta^{13}\text{C}$ relationship of pedogenic carbonate from northern China indicates a strong response of C_3/C_4 biomass to the seasonality of Asian monsoon precipitation. *Palaeogeogr. Palaeoclimatol. Palaeoecol.* 317–318, 32–40.
- Yang, S., Ding, Z., Li, Y., Wang, X., Jiang, W., Huang, X., 2015a. Warming-induced north-westward migration of the East Asian monsoon rain belt from the Last Glacial Maximum to the mid-Holocene. *Proc. Natl. Acad. Sci. U. S. A.* 112, 13178–13183.
- Yang, X., Jiang, W., Yang, S., Kong, Z., Luo, Y., 2015b. Vegetation and climate changes in the western Chinese Loess Plateau since the Last Glacial Maximum. *Quat. Int.* 372, 58–65.
- Zech, M., Pedentchouk, N., Buggle, B., Leiber, K., Kalbitz, K., Marković, S.B., Glaser, B., 2011. Effect of leaf litter degradation and seasonality on D/H isotope ratios of n-alkane biomarkers. *Geochim. Cosmochim. Acta* 75, 4917–4928.
- Zech, R., Zech, M., Marković, S., Hambach, U., Huang, Y., 2013. Humid glacials, arid interglacials? Critical thoughts on pedogenesis and paleoclimate based on multi-proxy analyses of the loess-paleosol sequence Crvenka, Northern Serbia. *Palaeogeogr. Palaeoclimatol. Palaeoecol.* 387, 165–175.
- Zech, M., Zech, R., Rozanski, K., Gleixner, G., Zech, W., 2015. Do n-alkane biomarkers in soils/sediments reflect the $\delta^2\text{H}$ isotopic composition of precipitation? A case study from Mt. Kilimanjaro and implications for paleoaltimetry and paleoclimate research. *Ios. Environ. Health Stud.* 51, 508–524.